OmegaCAM Commissioning - DFS - Illumination Characterisation and Correction

OmegaCAM Instrument Consortium

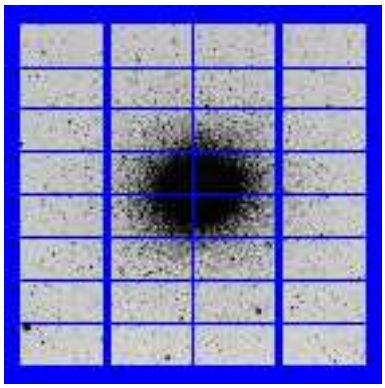

Document Number: VST-TRE-OCM-23100-3608

Issue Number: 2.1
Issue Date: July 4, 2012

Authors:

G. Sikkema
G. Verdoes Kleijn
E. M. Helmich
E. A. Valentijn
J. P. McFarland
D. R. Boxhoorn
J. Bout
H. Buddelmeijer
K. Kuijken
J. de Jong
E. Deul

Issued by: K. Kuijken

Distribution List

Recipient	Institute / Company	No. of Copies
D. Baade	ESO	1

Document Change Record

Issue	Date	Sect. / Paragr. affected	Reasons / Remarks
1.0	31.12.2011	all	first version
1.1	17.01.2012	rms table endresults completed	new results
2.0	02.05.2012	all	following feedback from ESO
2.1	04.07.2012	captions	corrected minor typos

1 Req 5.4.8/CP 8.17 - Cat II: Illumination correction

Required accuracy, constraints:

- OmegaCAM requirement R199 in the Verification Matrix in the OmegaCAM Technical Specifications (VST-SPE-ESO-23100-0002): to obtain 0.05 magnitudes photometric precision routinely over single science exposures, relative to the available standard stars.
- Goal for illumination Correction itself: better than 1% for the amplitude over a single CCD.

2 Characterization of illumination variations

To determine the variation in pixel sensitivity at any scale (from pixel-to-pixel scale via chip-to-chip scale to mosaic scale) for OmegaCAM, the Calibration Plan ensures that both twilight and dome flats are observed at least once a week. Twilights are observed at both dusk and dawn at varying rotator angles (recorded in header keywords ABSROT). Domeflats are observed during the day at a single, fixed rotator angle. Previous OmegaCAM commissioning reports (see especially VST-TRE-OCM-23100-3603, sections 14-17) have shown that twilight and dome flat exposures are both subjected to non-uniform illumination. Thus, the derivation of a 'true' flatfield (i.e., only the variation in pixel sensitivity) requires a correction on these illumination variations. This is termed illumination correction.

Figure 1 shows the photometric scale residual per chip for Sloan u,g,r,i and z if no correction for these illumination variations is applied. Within a chip the photometric scale residual varies by up to ~ 0.1 mag, bottom-to-peak. The large-scale residual pattern appears roughly point symmetric around the center of the mosaic. A variation in the stray light distribution which is point symmetric around the optical axis to first order can cause this. Other instruments show similar illumination variations patterns, i.e., having a central-axisymmetric 2D-polynomial shape (WFI: (Manfroid et al., 2001; Koch et al., 2004) and MEGACAM (Regnault, 2007)).

To determine an illumination correction for any flatfield, one needs to determine how the illumination variation itself varies as a function of flatfield observational parameters (date-obs, rotator angle etcetera). Previous OmegaCAM commissioning reports (VST-TRE-OCM-23100-3603 / 3605 / 3607) have shown that the ratio of twilight and domeflat exposures is twilight-flat rotator angle dependent to a level of $\sim 10\%$ (from peak-to-valley over the whole mosaic) for g,r,i and z. Also for domeflats a dependence on rotator angle is present, but smaller ($\sim 5\%$). The continuous variation in flat field appearance as a function of rotator angle for both twilight and dome flats (see VST-TRE-OCM-23100-3607, section 13) suggests that rotator angle is the dominant (if not only) dependency that sets the illumination variation pattern. Support for this hypothesis is strengthened by an analysis of 5 months of OmegaCAM twilight and dome flat observations (September 2011 to February 2012). The twilight flatfield movie attached to this report shows the residual between a single twilight flat field and the mean of all twilight flatfields ordered by rotation angle. Again, the flatfield appears to change in a regular fashion with rotator angle. Figure 2 shows that the domeflats over the same 5 months, all observed at a fixed rotator angle, show very little variation: only at levels of $\sigma \sim 0.2\%$ or lower for g, r and i and only at a spatial scale of pixel-to-pixel. Such constant domeflats imply that the relative pixel sensitivities (and illumination variation in domeflats) vary maximally to this level, over this timespan. **The conclusion is that the intrinsic flat field (i.e., pixel sensitivities) can be considered constant with respect to requirement R199 from spatial scales starting at pixel-to-pixel up to full CCD size.** The interpretation is that this conclusion on intrinsic flatfield holds also for the Sloan u filter. Figure 2 shows significantly more variation for the Sloan u domeflat. The domelamps are extremely weak in u (see VST-TRE-OCM-23100-3605). Hence the dome flat in u is dominated by scattered light. The interpretation is that the scattered light distribution apparently varies over time. The solution is to use only twilight flats for u to determine the illumination correction. As shown later, this approach is validated by the performance of the illumination correction in u.

Therefore it was decided to build for the Sloan g,r,i and z filter a single masterflat from a combination of a single twilight flat and single dome flat and apply this to all OmegaCAM observations used to determine and test the illumination correction (Table 1). (For u only the

twilight flat is used.) In terms of intrinsic pixel sensitivities, the constancy of the domeflats indicates such a fixed masterflat is applicable to observations over a wide timespan. The usage of a single flat (i.e., at single rotator angle) simplifies the procedure: a single illumination correction needs to be derived. The masterflat is constructed in Fourier space: frequencies corresponding to large scales / small scales are taken from the twilight / dome flat, respectively.

3 Illumination Correction

3.1 Observational input data

Precise calculation of an illumination correction over the 32 2K $\times$ 4K CCDs requires hundreds of reference sources per CCD. For that reason, dedicated observations were made of standard star fields covered by the SDSS DR7 catalog (Abazajian et al. 2009). DR7 is photometrically highly uniform and homogeneous and therefore stars in the DR7 catalog can be used as photometric reference catalog. SA92, SA95 and SA113 were selected and observed in all key bands under photometric conditions during COMM3 (see Table 1). The SA fields were observed at 33 (or 37) dithers positions. 32 of these dither positions are single-chip offsets such that a group of stars is observed on all 32 CCDs. For each chip the sources extracted from the 33 (or 37) observations are combined in a single catalog of unsaturated sources. This catalog is associated with a filtered DR7 catalog: only point sources (SDSS flag=6) that are brighter than 19.0, 19.0, 18.8, 18.5 and 17.7 in u,g,r,i and z respectively. The resulting catalog contains for each source: the pixel coordinates, the reference magnitude and the extinction corrected instrumental magnitude. The photometric scale residual is defined as the difference between the latter two. A zeropoint per chip is computed as the average of the photometric scale residuals after applying a 2-sigma clipping. The magnitude residuals, i.e., the difference between the zeropoint and reference magnitude, sample the illumination variations. To get more signal, all residual magnitudes for the three SA fields, SA92, SA95 and SA113 were combined to end up with roughly 1000 objects per chip for g, r, i ,z and about 500 for the u-band.

3.2 Global illumination correction

To assess the large-scale illumination variation for OmegaCAM it was modeled as an 2nd degree central-axisymmetric 2D-polynome (see Figure 2 to 5 of VST-TRE-OCM-23100-3607). This model was fitted to the 32 catalogs and simultaneously 32 individual zeropoints, one for each CCD was fitted.

The fitted illumination correction corrects the large-scale illumination. However, the magnitude residuals still show local off-sets that are larger than requirement R199 in horizontal strips along gaps (see Fig. 3). Smaller off-sets are visible in the corners and the central regions of the focal plane. To solve simultaneously for not only the large-scale variations but also these local deviations, a more localized determination is required needed for the illumination correction. The local solution should determine the illumination correction in areas having sizes equal to the smallest deviant structures seen in the residual plot of the polynome model: Figure 3 (taken from VST-TRE-OCM-23100-3607).

3.3 Localized Illumination Correction

The calculation of the localized Illumination Correction (IC) involves several steps. The IC corrects for illumination variations of a given flatfield. In other words, each IC model always depends directly on the flatfield applied. This implies that the science data need to use the same flatfield as was used to calculate the IC model. Throughout this report it is important to note that all derived IC models mentioned in this report were always derived with the default twilight flatfield, listed in the first part of Table 1. Tests will also be done, applying these IC models on science data reduced with a twilight flatfield, rotated w.r.t. the default flatfield (see second part of Table 1).

Table 1: Observations used to determine illumination corrections: from top to bottom: first part: default twilight flatfield; second part: twilight flatfield at different rotator angle (ABSROT); third part: SA92, 95 and 113 dithered observations; fourth part: KiDS-N fields. Template.start: to identify observations: starting date of observing template. ABSROT: range in rotator angle within observations in observing template (deg). ALT/AZ: ranges in altitude and azimuth within observing template. During the period spanned by these observations one technical intervention on the OmegaCAM+VST system took place: 6-10 January 2012. It was restricted to VST.

Object	Filter	Template.Start	ABSROT (deg)	ALT (deg)	AZ (deg)
default dome flat	g	2011-08-05 14:53:45	-	-	-
default dome flat	r	2011-08-07 11:02:08	-	-	-
default dome flat	i	2011-08-05 15:02:50	-	-	-
default dome flat	z	2011-10-21 09:39:40	-	-	-
default tw. flat	u	2011-08-05 22:35:06	58 - 56	74-74	243-241
default tw. flat	g	2011-08-10 22:36:23	-27 - -34	85-85	152-145
default tw. flat	r	2011-08-10 22:41:36	-47 - -53	85-84	131-125
default tw. flat	i	2011-08-17 22:37:07	-65 - -67	81-80	112-109
default tw. flat	z	2011-10-20 22:58:00	65 - 63	79-80	249-247
rotated tw. flat	u	2011-10-03 22:52:13	76 - 76	63-64	267-266
rotated tw. flat	g	2011-10-18 23:10:14	-41 - -38	79-80	136-140
rotated tw. flat	r	2011-08-13 22:45:18	26 - 19	81-81	207-200
rotated tw. flat	i	2011-08-05 22:40:38	55 - 53	75-76	239-238
rotated tw. flat	z	2011-08-07 22:37:20	-94 - -94	65-64	73- 73
SA92	u	2011-08-11 08:29:58	55 - 34	42-60	245-218
SA95	u	2011-08-07 07:06:01	39 - 02	56-65	224-182
SA113	u	2011-08-05 06:10:10	-21 - -49	63-50	157-124
SA92	g	2011-08-05 07:54:37	24 - -04	62-65	207-176
SA95	g	2011-08-12 08:55:28	51 - 35	48-59	239-220
SA113	g	2011-08-04 07:55:29	-51 - -59	47-36	121-110
SA92	r	2011-08-07 08:46:01	55 - 44	42-55	245-230
SA95	r	2011-08-12 06:21:53	45 - 21	53-63	231-203
SA113	r	2011-08-04 06:49:44	-35 - -51	59-48	141-121
SA92	i	2011-08-10 06:16:43	48 - 16	50-64	235-198
SA95	i	2011-08-10 08:36:05	55 - 33	43-60	244-217
SA113	i	2011-08-06 07:07:27	-43 - -58	55-38	132-111
SA92	z	2011-08-11 06:38:28	42 - 15	55-64	227-197
SA95	z	2011-08-06 08:38:48	57 - 46	40-53	247-233
SA113	z	2011-08-07 05:49:34	-14 - -40	64-57	164-135
KiDS-N KiDS_135.0_0.5	u	2012-01-25 06:25:54	-24 - -30	65-63	154-146
KiDS-N KiDS_139.0_-1.5	g	2012-01-26 06:20:15	-23 - -30	65-63	155-147
KiDS-N KiDS_139.0_-1.5	r	2012-02-29 04:33:25	-34 - -43	62-57	142-131
KiDS-N KiDS_135.0_0.5	i	2011-12-22 06:57:04	22 - 13	63-64	204-194

After the reduction stage: flatfielding and de-biasing (and de-fringing in i) the science frames, these are the dedicated 33 dithered observations of three SA fields and several KiDS-N fields (Verdoes Kleijn et al., 2012), the next steps are: source extraction (catalog construction) and filtering of the objects (see Section 3.1), determination of the Voronoi bins,and construction of the illumination frames by 2D-interpolation across Voronoi cells. Below, a detailed description is given for the last two of these steps, valid for each single chip.

- Binning + Voronoi cells
  Voronoi binning is a 2D binning technique, meant to reach a similar S/N in each bin, or in more formal words: it is an adaptive spatial binning method. The method is described in Cappellari & Copin (2003)

and a variety of its applications can be found in Cappellari (2009). The (IDL) code is freely available [1]. The code was slightly modified to make it more automatic and to remove unnecessary features.
The Voronoi software groups the pixels into Voronoi cells depending on signal+noise of those pixels (examples: Figure 9 and 10 of Cappellari & Copin 2003). The signal in a pixel is just the number of objects present in that pixel. Most of the times this is zero: remember 1000 'signals' are spread over ≈ 2000x4000=8 million pixels. For performance reasons, the image is re-binned into 30 (x direction) x 60 (y direction) = 1800 'pixels'. This gives on average roughly 0.5 object within each 'pixel'. The signal in each 'pixel' is defined as the number of objects present in that 'pixel', while the noise is just the square root of the number of objects in that 'pixel'. For u, g, r, i and z the signal (number of objects) in each Voronoi cell was set at 9, 13, 13, 16 and 16. The software then calculates a Voronoi cell distribution, with each Voronoi cell having a varying the shape and size depending on the signal and each Voronoi cell containing a list with objects present in that cell. Finally the un-weighted average of the magnitude residuals of the objects present in each Voronoi cell was calculated: this is the value of that particular Voronoi cell. The output is a list of 'pixel' coordinates of the centers of the Voronoi cells plus their values. After de-binning the central Voronoi coordinates to the original pixel scale, the resulting data is used in the following step, the Delaunay interpolation.

- Interpolation: Delaunay Triangulation
A continuous illumination variation map is obtained by interpolating between Voronoi cells. Voronoi cells are well suited to apply a Delaunay triangulation. This triangulation linearly interpolates between the Voronoi cells (examples: Figure 9 and 10 of Cappellari & Copin 2003). For the border regions of the chip, interpolation was done by mirroring the Voronoi cells. Next, the IDL code was applied that calculates the Delaunay triangulation between Voronoi cells. The code also produces the final products: the illumination correction frames as used in the remainder of this report and Astro-WISE. These frames are visible in the focal plane at the bottom of Figures 5, 7, 9, 11 and 13 for u,g,r,i and z respectively.

Table 2: **Illumination Correction Results**. Standard deviations of residual magnitudes in the five SLOAN filters left after applying the localized illumination corrections. The internal and external standard deviation (sd) of the magnitude residuals are defined as follows: external is with respect to the stellar reference magnitude in the standard star catalog (SDSS DR7 stellar photometry). Internal is w.r.t. the mean of its observed magnitudes. 2nd and 3rd column: sd of internal and external errors if only zero points are applied; 4th and 5th columns: sd of internal and external errors when illumination correction applied on derivation data (SA92+SA95+SA113); 6th and 7th columns: sd of internal and external errors when illumination correction applied on SA113 data reduced with a twilight flatfield rotated ROTANG degrees (8th column); 9th and 10th columns: sd of internal and external errors when illumination correction applied on KiDS north data reduced with the default twilight flatfield

	zp only	zp only	SAs	SAs	ff. rot	ff. rot	ff. rot	KiDS	KiDS
(1)	(2)	(3)	(4)	(5)	(6)	(7)	(8)	(9)	(10)
band	sd_int	sd_ext	sd_int	sd_ext	sd_int	sd_ext	Δ rot	sd_int	sd_ext
u	0.029	0.036	0.017	0.029	0.017	0.031	-19	0.013	0.025
g	0.020	0.030	0.010	0.020	0.010	0.022	9	0.009	0.024
r	0.021	0.029	0.009	0.021	0.010	0.022	-73	0.012	0.022
i	0.022	0.030	0.012	0.022	0.012	0.023	-118	0.010	0.024
z	0.027	0.033	0.015	0.027	0.016	0.028	158	-	-

3.4 Results

In this section, the derived illumination correction (IC) model is applied to three different datasets. First, the IC model is applied to the same dataset from which the illumination correction was derived, i.e. the combination of data SA92, SA95 and SA113. The second dataset consists of the SA113 data reduced with

[1] http://www-astro.physics.ox.ac.uk/ mxc/idl/#binning

other, rotated, twilight flatfields. Third, the IC model is applied to KiDS-N science data (Verdoes Kleijn et al., 2012) that overlaps with SLOAN DR7 data. The IC is applied in the following way: after de-biasing, flatfielding and optionally, de-fringing, the background is determined and subtracted using SWARP (Bertin et al., 2002). The resulting image is then just divided by the IC model. Table 2 quantifies the results for the three different data sets. This table lists standard deviations of internal and external errors. Internal errors are the errors w.r.t. the mean of the observed magnitudes per star. External is with respect to the stellar reference magnitude in the standard star catalog, which is SDSS DR7 photometry in this case. Note that if only zeropoints are applied, like in Figure 3, the requirement is already met (see 2nd and 3rd columns listing the internal and external errors if only zeropoints are applied). However, from Figure 3, spatial dependencies on magnitude error are visible. The localized IC model should correct for that.

- Illumination correction on same data
  Figures 5, 7, 9, 11 and 13 show similar plots as the OCAM3 report for the polynome approach. They represent 2D maps of the OmegaCAM 32 ccds combined field of view, in pixel coordinates. The datapoints in the four top panels of each plot represent all DR7 reference stars of SA92, SA95 and SA113 after dithering 33 times and filtering (see above). The bottom three panels have a color scale from -0.06 to +0.06 magnitude. Data points are enlarged in such a way to fill up gaps but to minimize overlap of the data points. The top left panel shows the raw zeropoints for all SDSS DR7 reference stars, with raw zero point defined as the reference magnitude minus the extinction corrected instrumental magnitude. The top right panel shows the complete model, i.e. fitted zeropoints per chip + illumination variation model. The illumination variation model alone is shown middle left. The residual magnitudes of reference stars after applying the full model (zeropoints + illumination correction) is shown middle right. At the bottom the illumination variation model is shown. The residual-magnitudes plot shows that the local deviations (horizontal strips) have vanished. Another way to visualize the magnitude residuals is to plot a histogram. This is shown in the top left panel of Figures 6, 8, 10, 12 and 14 (the top right panel of these Figures is just a copy of the residual plots). To quantify the spread of the histograms, the standard deviation of the residuals was calculated. These values for all bands are visible in column 5 of Table 2. The standard deviations of the internal errors are halved with respect to the situation when only zeropoints are applied, the external errors are reduced by about a third. It is clear that these error margins lie well below the requirement of 0.05 mag.

- Illumination correction on data reduced with a rotated twilight flatfield.
  In this section, the results are discussed of SA113 data (Table 1), flatfielded using a twilight flat that was rotated w.r.t. the default twilight flatfield. The relative rotation angles are listed in column 8 of the Table 2. The residual magnitudes are shown in the middle panels of Figures 6, 8, 10, 12 and 14, after applying the IC model. The right panel shows residual magnitudes in the focal plane in pixel coordinates, while the left panel shows the corresponding histogram of these off-sets. Compared with the top panels, the maps of the residual magnitudes looks less smooth. This is also visible in the histograms: these are wider than the top panels for all bands, suggesting larger errors. This is quantified in Column 7 of Table 2, which lists the standard deviation of these histograms in each band. Although the errors are larger than before, the values demonstrate that for all bands the standard deviation is within the requirement of 0.05 magnitude.
  Comparing Column 7 with column 5, it shows that the differences between these columns are lower than 0.01 magnitude for all bands. Or in other words: the illumination correction model seems to be stable at the 1% level when it is applied to science data reduced with a twilight flatfield with a relative rotation angle.

  The main result is that the horizontal strips, visible when using the polynome approach, have vanished. The residual magnitudes maps do show local magnitude offsets.
  Although the standard deviations still have dramatically improved compared to no IC, the local off-sets caused by the relative rotated twilight flatfield, will disturb the photometry of a co-added frame. Therefore, it is desirable to use the same twilight flatfield for all reductions. This is what also, currently as of April 2012, is done for the KiDS project (Verdoes Kleijn et al., 2012) .

- Illumination correction on KiDS-N science data

Some pointings of the KiDS survey (Verdoes Kleijn et al., 2012) overlap with Sloan DR7 data. This enables us to directly compare the photometry of science data, reduced with the default flatfields and illumination correction. All KiDS pointings analyzed here (see Table 1) have been observed after the VST intervention of 6-10Jan 2012, while the data on which the illumination correction is based were observed months prior to the intervention.

The analog of the procedure applied to the dithered SA observations is applied to the KiDS fields. The dithered KiDS observations allow to measure the same star at 5 different locations in the focal plane. However instead of dithering 33 times with Δx$\approx$2000 and Δy$\approx$4000, there are now only 5 dithering steps with offsets $\approx$ 100 pixels, causing the large majority of the stars ending up five times on the same chip. In this manner, for each band, one particular KiDS field was compared with DR7 data (see fourth part of Table 1). Columns 9 and 10 of Table 2 show the standard deviations of the internal and external residuals and Figures 6-12 and 4 show the external residuals distributions. The residuals magnitudes seem comparable to those of the SA fields. The differences are mainly caused by sparsity of the data due to the different observing mode: here only 5 dithers are available, with very small dither steps compared to the 33 (37) pointing dithers.

3.5 Conclusions & considerations

Conclusions:

- OmegaCAM requirement R199 in the Verification Matrix in the OmegaCAM Technical Specifications (VST-SPE-ESO-23100-0002)has been met: to obtain 0.05 magnitudes photometric precision routinely over single science exposures, relative to the available standard stars. The goal for characterizing illumination correction itself has also been met: better than 1% for the amplitude over a single CCD, (see OmegaCAM DFS User Requirements, VST-SPE-OCM-23100-3050)
- OmegaCAM illumination variations consist of localized components (especially near the covers over the detector heads) and a global component varying on the scale of the full mosaic. The illumination variations are also rotator angle dependent.
- The correction method presented here corrects for both components because it characterizes the illumination variations on small enough spatial scales. It overcomes the rotator angle dependence by virtue of the stability of the intrinsic ("true") flatfield. This allows the correction to be determined for a single master flatfield created out of dome and twilight flats at fixed rotator angles.
- The determined illumination correction remains accurate on timescales of at least 7 months of OmegaCAM survey operations. A period that included a VST technical intervention.
- Usage of illumination correction by ESO and its user community: the u,g,r,i and z masterflats and illumination correction frames are made publicly available by the OmegaCAM commissioning team. They can be retrieved from the Astro-WISE system.

Considerations:

- The OmegaCAM team monitors for changes in the OmegaCAM illumination variation by monitoring both domeflats and twilight flats. **We re-iterate our recommendation to ESO to observe also twilight flats at fixed rotator angle.** It makes monitoring of the illumination correction, and updating as needed, much better doable and traceable as the observational setup evolves gradually or changes abruptly (e.g., technical interventions).
- The illumination correction approach here can account for the sub-percent changes in pixel-to-pixel sensitivity over time. This is done by updating the domeflat that goes into the illumination correction.

- Science images are generally observed at a rotator angle that differs from the flatfield. Thus, the correction applied is valid for sources that are small compared to the scale over which illumination variation is significant. Extended surface brightness distributions on scales of a CCD or larger in science exposures can still contain some imprint of illumination variations. This can amount to 0.04mag maximally. The correction approach allows to make a science exposure-specific illumination correction by using a twilight with the same rotator angle as the science image in the illumination correction.

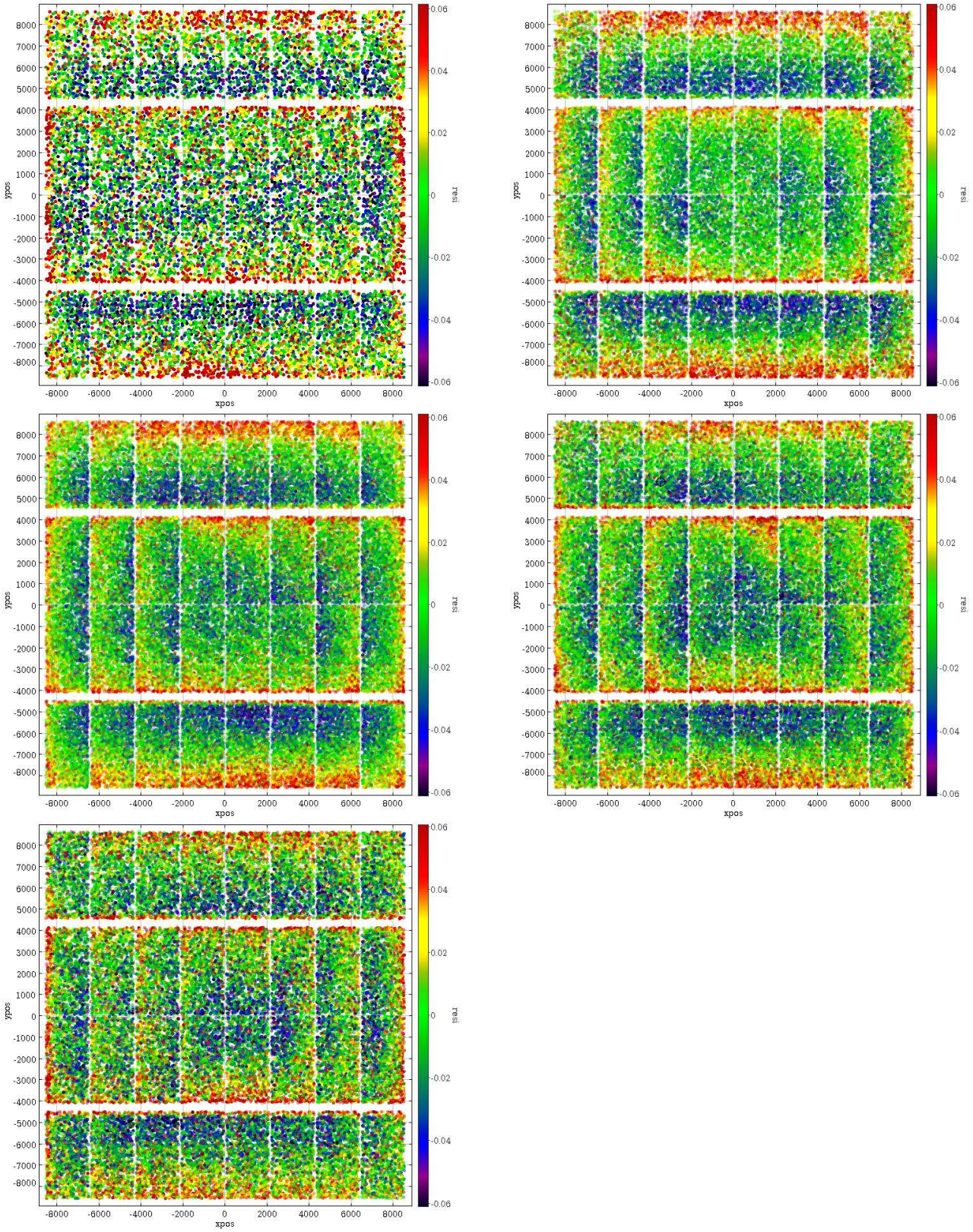

Figure 1: Photometric residual of stars in SA113 after subtraction of an individual zeropoint per chip. Top-left to bottom-right: Sloan u,g,r,i and z. Residuals are computed using magnitudes for stars listed in the SDSS DR7 catalog (see Section 3.1 for details of stellar selection criteria). The flatfields applied are identical to those used in determining illumination corrections presented in this report.

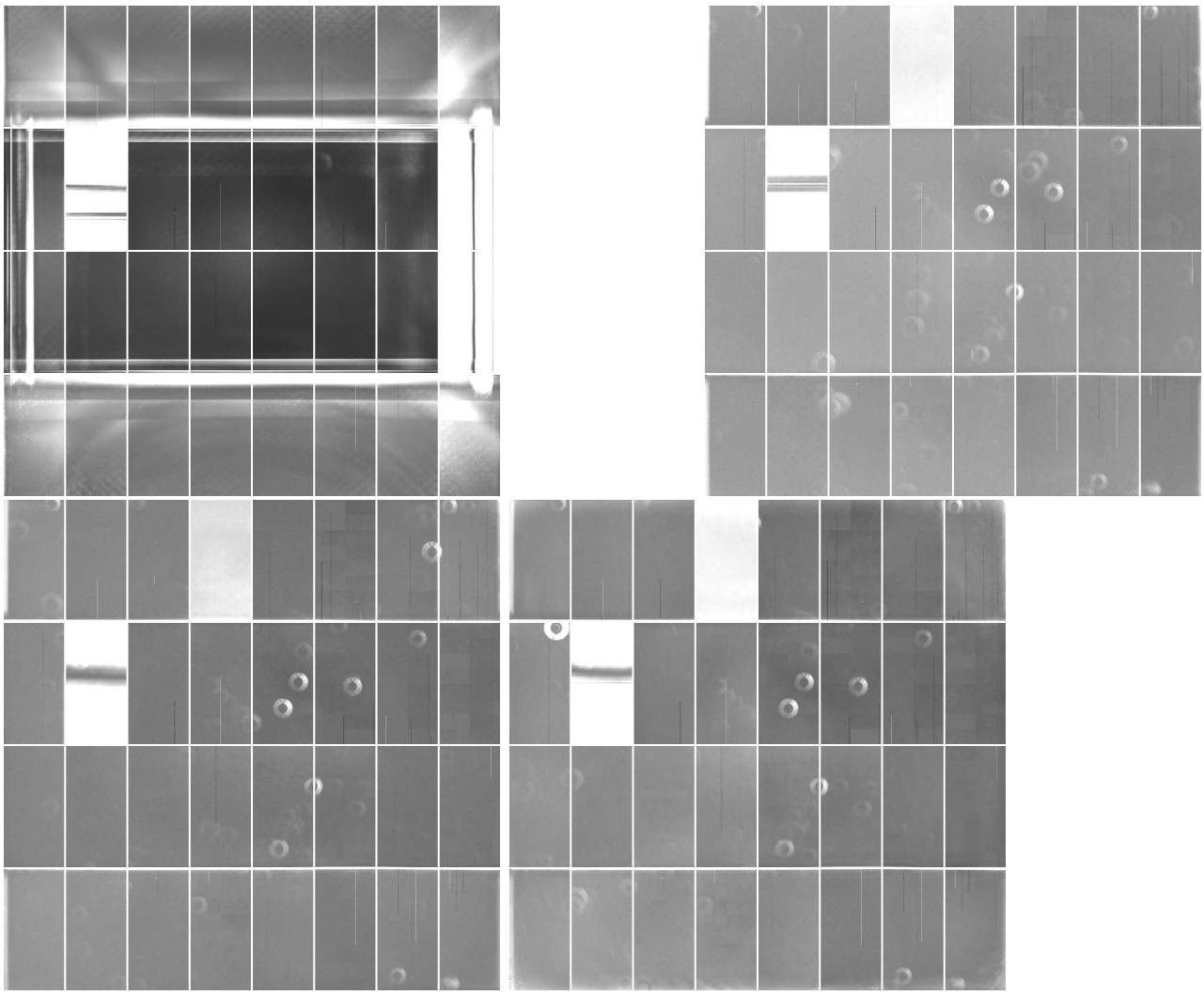

Figure 2: Stability of domeflats. Standard deviation images of domeflats for u, g, r and i (top-left to bottom-right) over a period of 5 months (September 2011 - February 2012). The color scaling black → white corresponds to standard deviation of 0.0010→0.0016. Domeflats are variable at a level below 0.2% over many months. The exception are 2 CCDs (#82 and #92) which are known to have instabilities such as varying gain levels. The constant domeflats imply that pixel sensitivities and illumination variation vary at a level below 0.2% in domeflats over months.

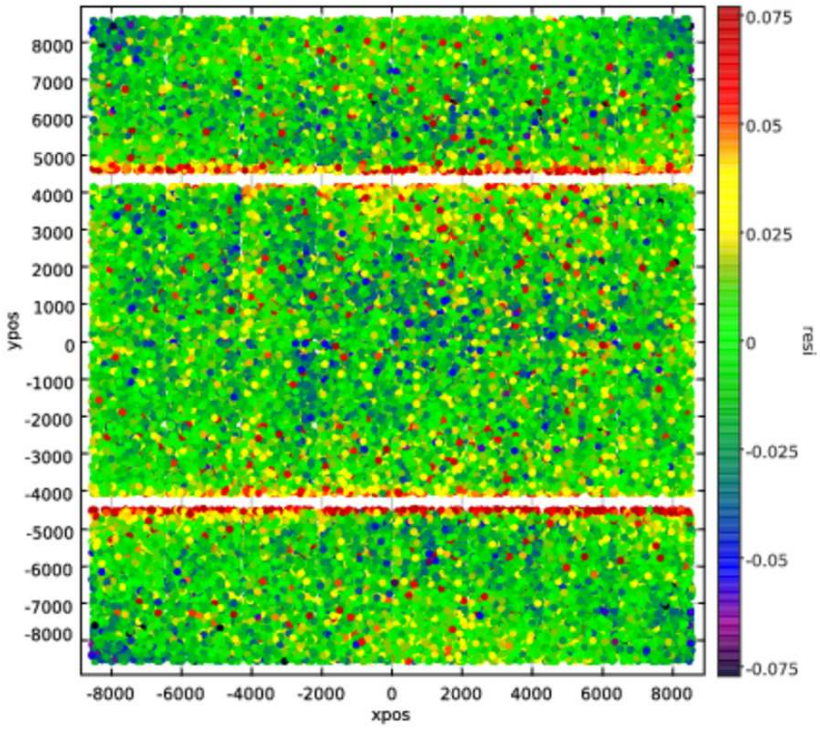

Figure 3: The r-band magnitude residuals of the reference stars after modeling with one 2D-polynomial + 32 ZPTs as free parameters. Local deviations from zero are visible. Residuals are computed using magnitudes for stars listed in the SDSS DR7 catalog.

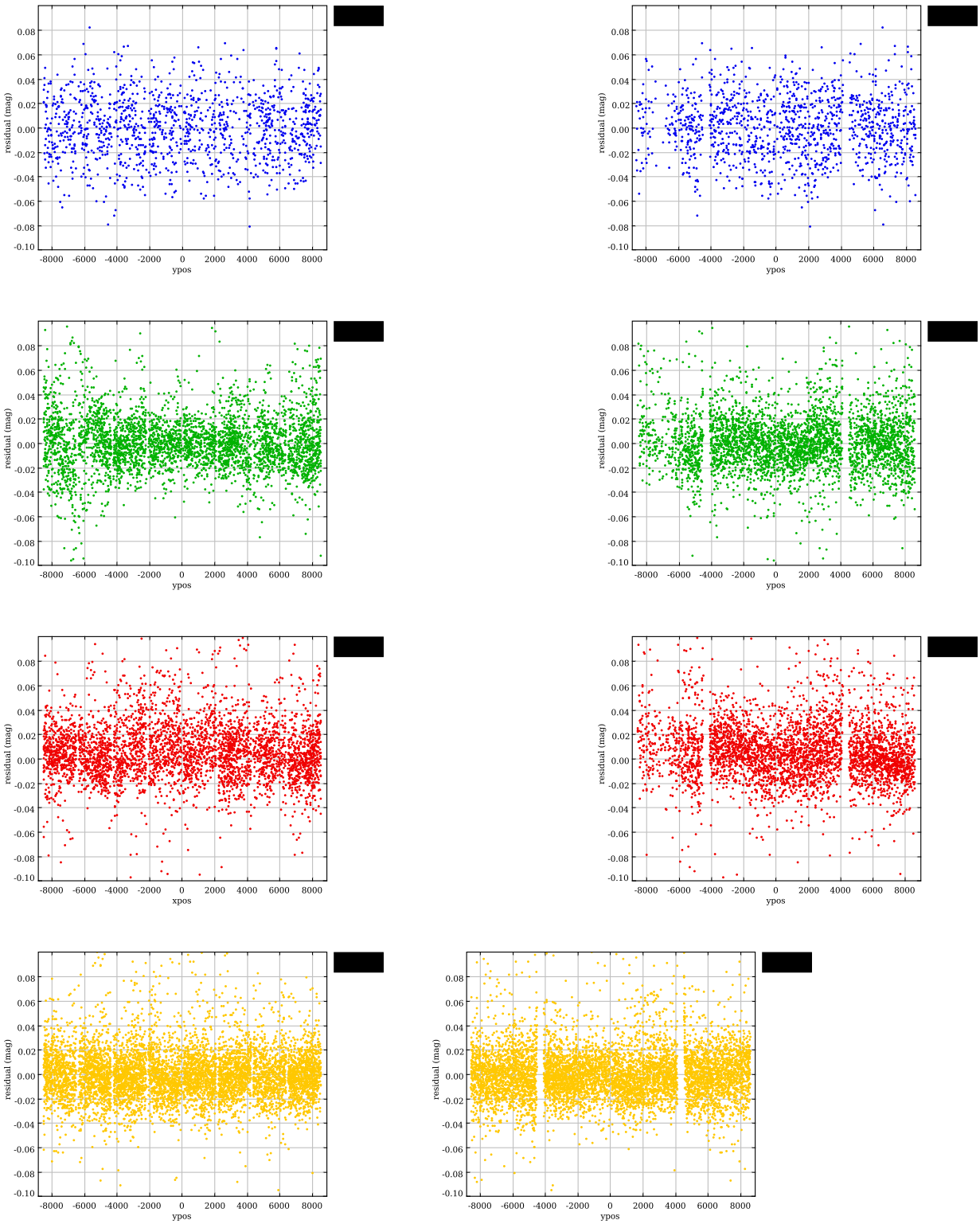

Figure 4: Magnitude residuals for stars in the KiDS-N fields listed in Table 1 and their magnitudes in the SDSS DR7 catalog versus location in the detector plane. Left/right column: versus X/Y respectively. Top to bottom row: Sloan u,g,r and i. The photometry for each individual step of the 5/(4) dither steps for g,r,i/(u) observations is plotted together.Filtering applied for star selection is identical as used in determining illumination corrections.

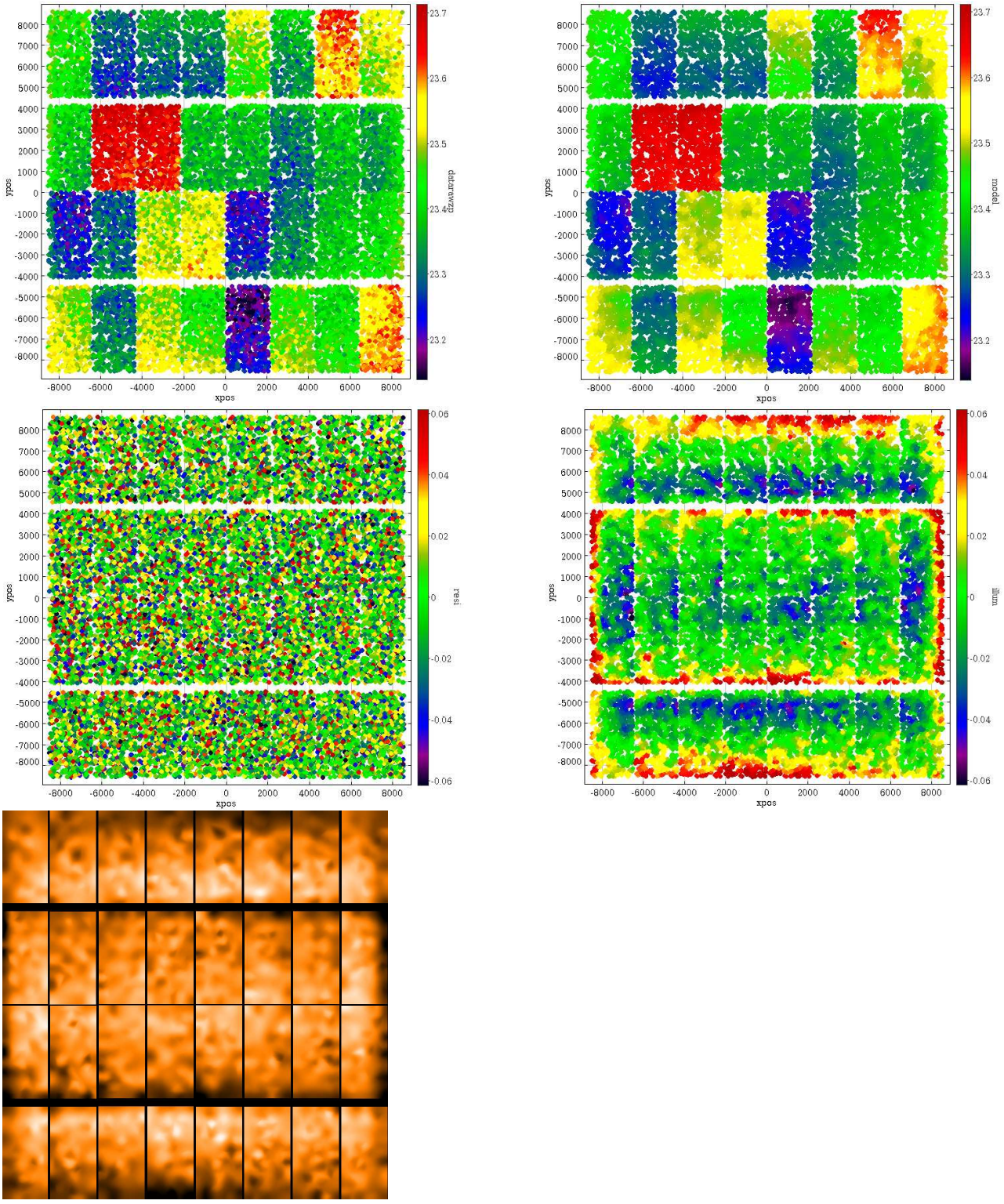

Figure 5: Illumination correction results for Sloan u projected on the focal plane. The datapoints in the top four plots represent all DR7 reference stars of SA92, SA95 and SA113 after dithering 33 times and filtering (see text). Bottom three plots have a color scale from -0.06 to +0.06 magnitude. Data points are enlarged in such a way to fill up gaps, overlapping datapoints should be minimal. Top left: raw zeropoints for all SDSS DR7 reference stars. Top right: model = fitted zeropoints per chip + illumination variation model. Middle left: residual magnitudes of reference stars after applying illumination correction. Middle right: illumination variation model (i.e. with ZPT per chip subtracted). Bottom: full illumination correction model .

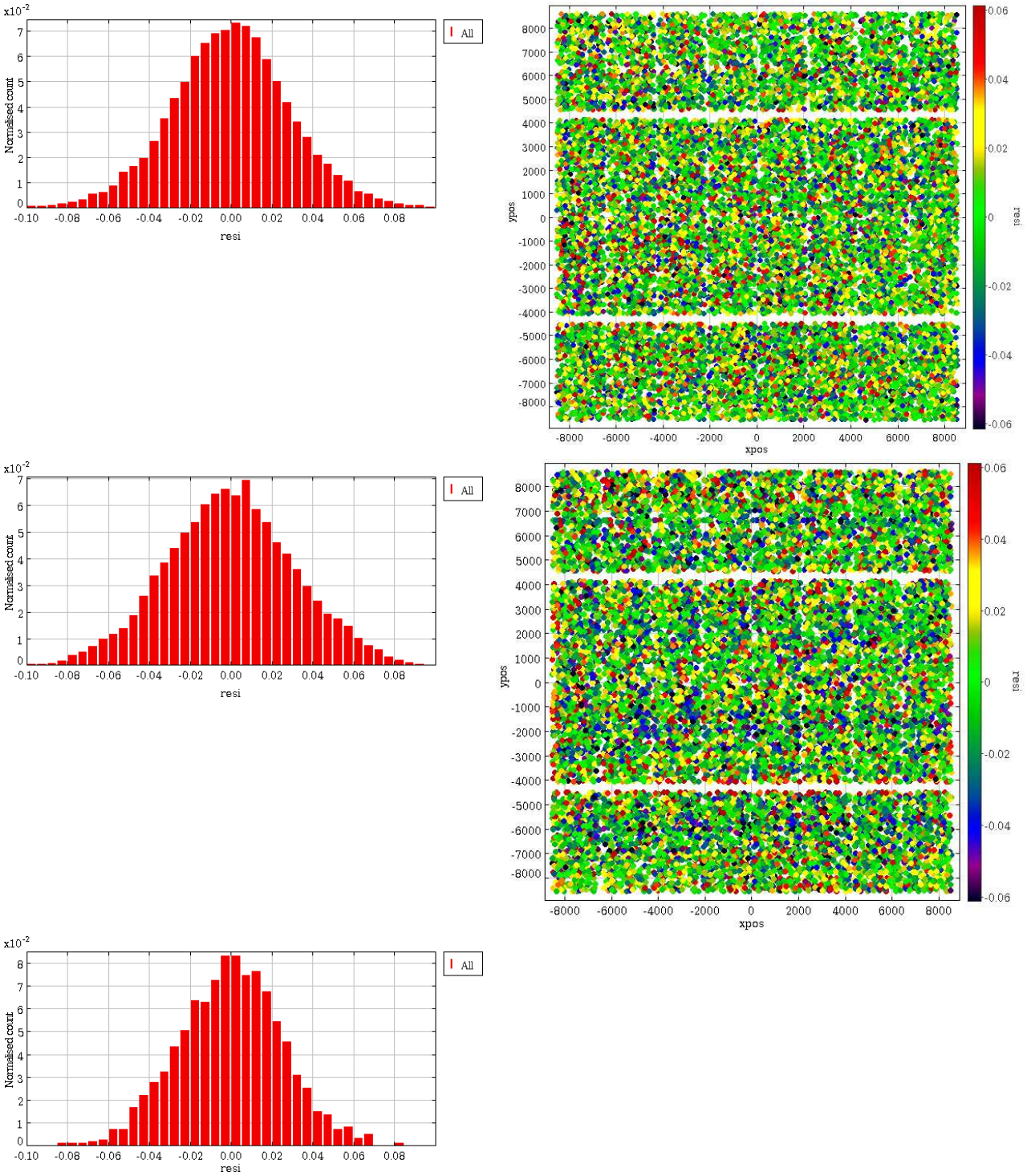

Figure 6: Illumination correction results u band: Top left and right: histogram and focal plane map of residual magnitudes after applying illumination correction on data itself (combination of SA92, SA95 and SA113). Middle: same plots for SA113-data reduced with twilight flatfield rotated -19 degrees compared to the flatfield used to derive the illumination correction. Bottom: same as top plots before but now for KiDS_135.0_0.5 with template start 2012-01-25 06:25:54 reduced with the same flatfield as the illumination correction (KiDS-mode).

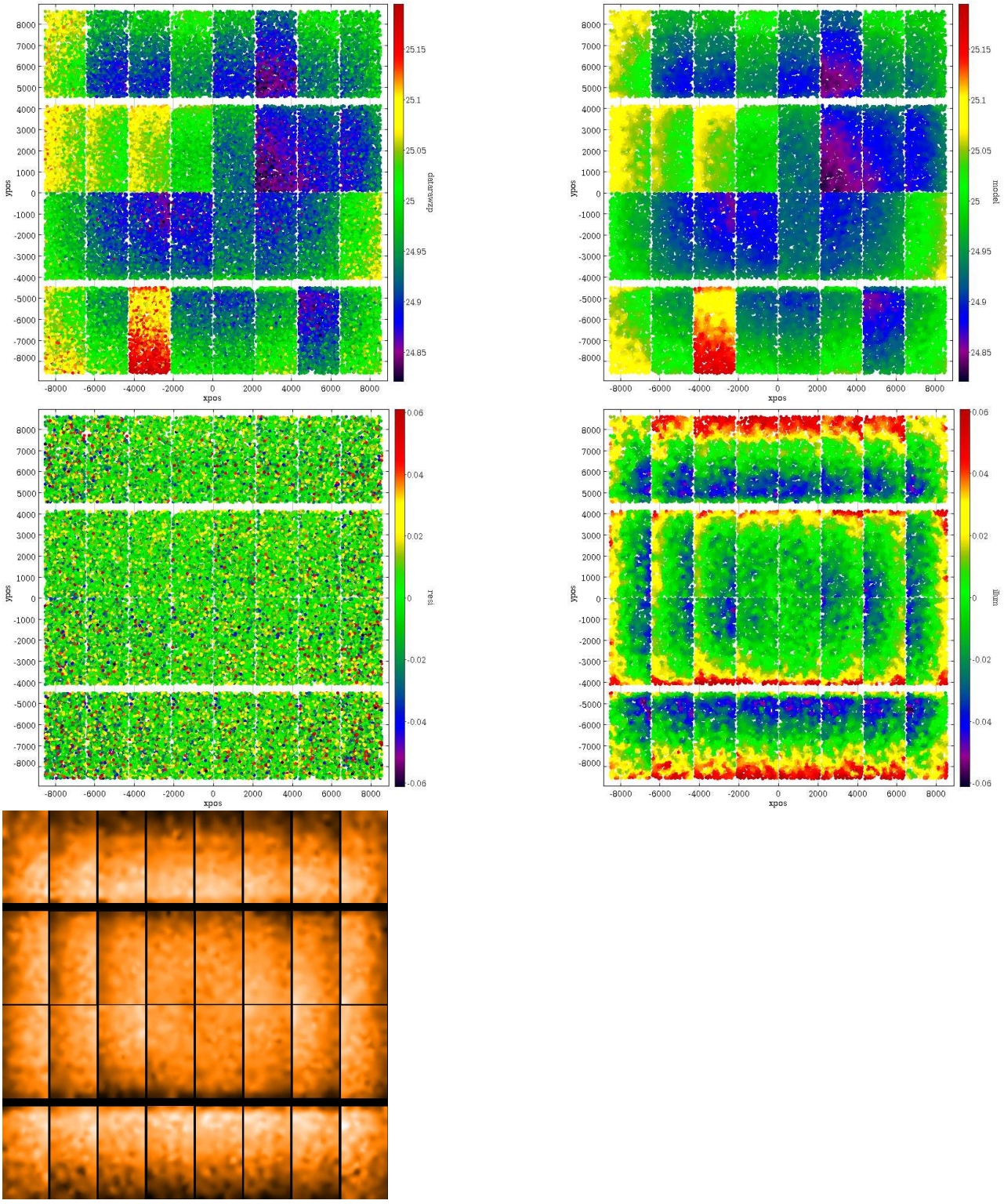

Figure 7: Illumination correction results for Sloan g projected on the focal plane. The datapoints in the top four plots represent all DR7 reference stars of SA92, SA95 and SA113 after dithering 33 times and filtering (see text). Bottom three plots have a color scale from -0.06 to +0.06 magnitude. Data points are enlarged in such a way to fill up gaps, overlapping datapoints should be minimal. Top left: raw zeropoints for all SDSS DR7 reference stars. Top right: model = fitted zeropoints per chip + illumination variation model. Middle left: residual magnitudes of reference stars after applying illumination correction. Middle right: illumination variation model (i.e. with ZPT per chip subtracted). Bottom: full illumination correction model .

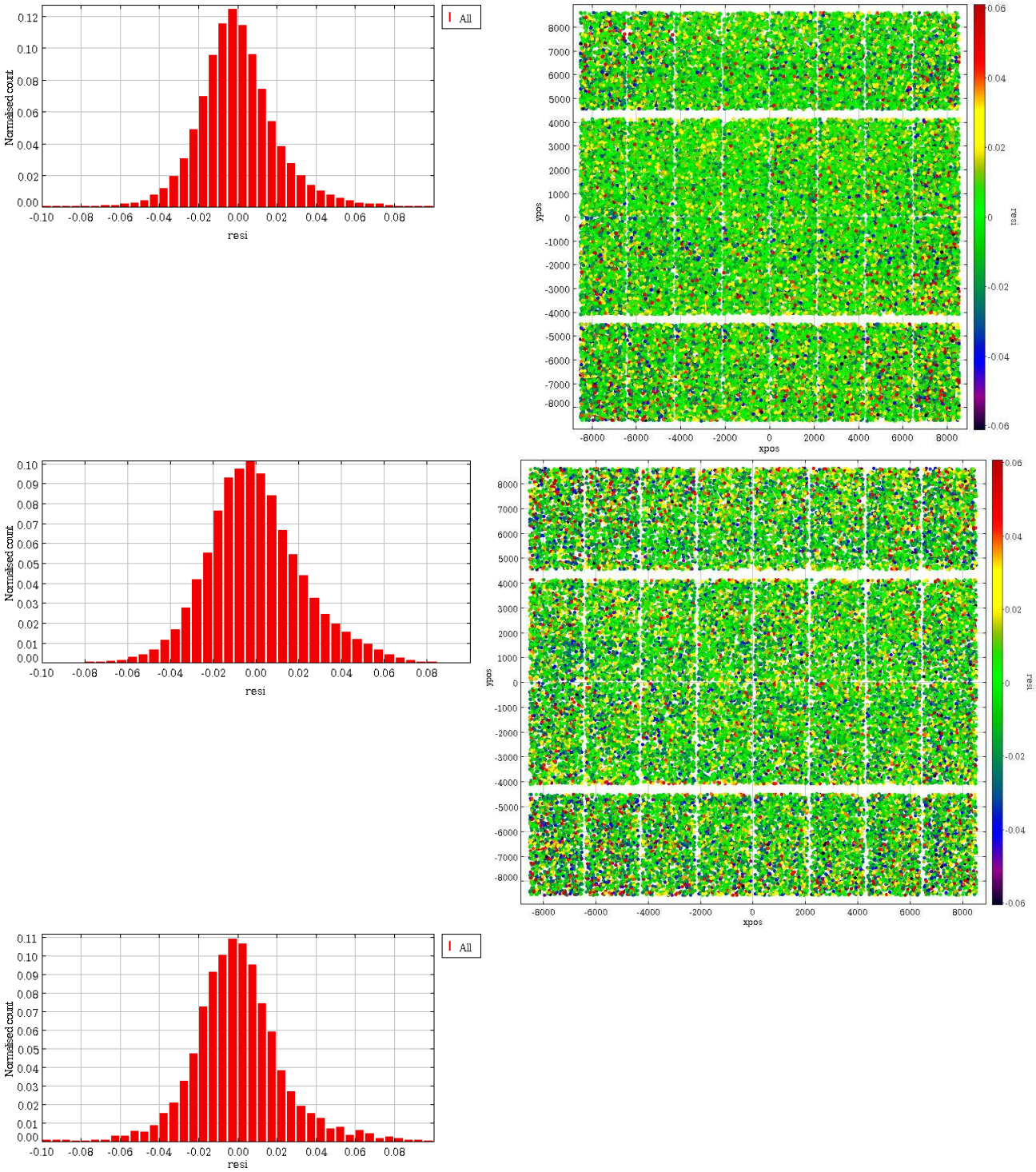

Figure 8: Illumination correction results g band: Top left and right: histogram and focal plane map of residual magnitudes after applying illumination correction on data itself (combination of SA92, SA95 and SA113). Middle: same plots for SA113-data reduced with twilight flatfield rotated 9 degrees compared to the flatfield used to derive the illumination correction. Bottom: same as top plots before but now for KiDS_139.0_-1.5 with template start 2012-01-26 06:20:15 reduced with the same flatfield as the illumination correction (KiDS-mode).

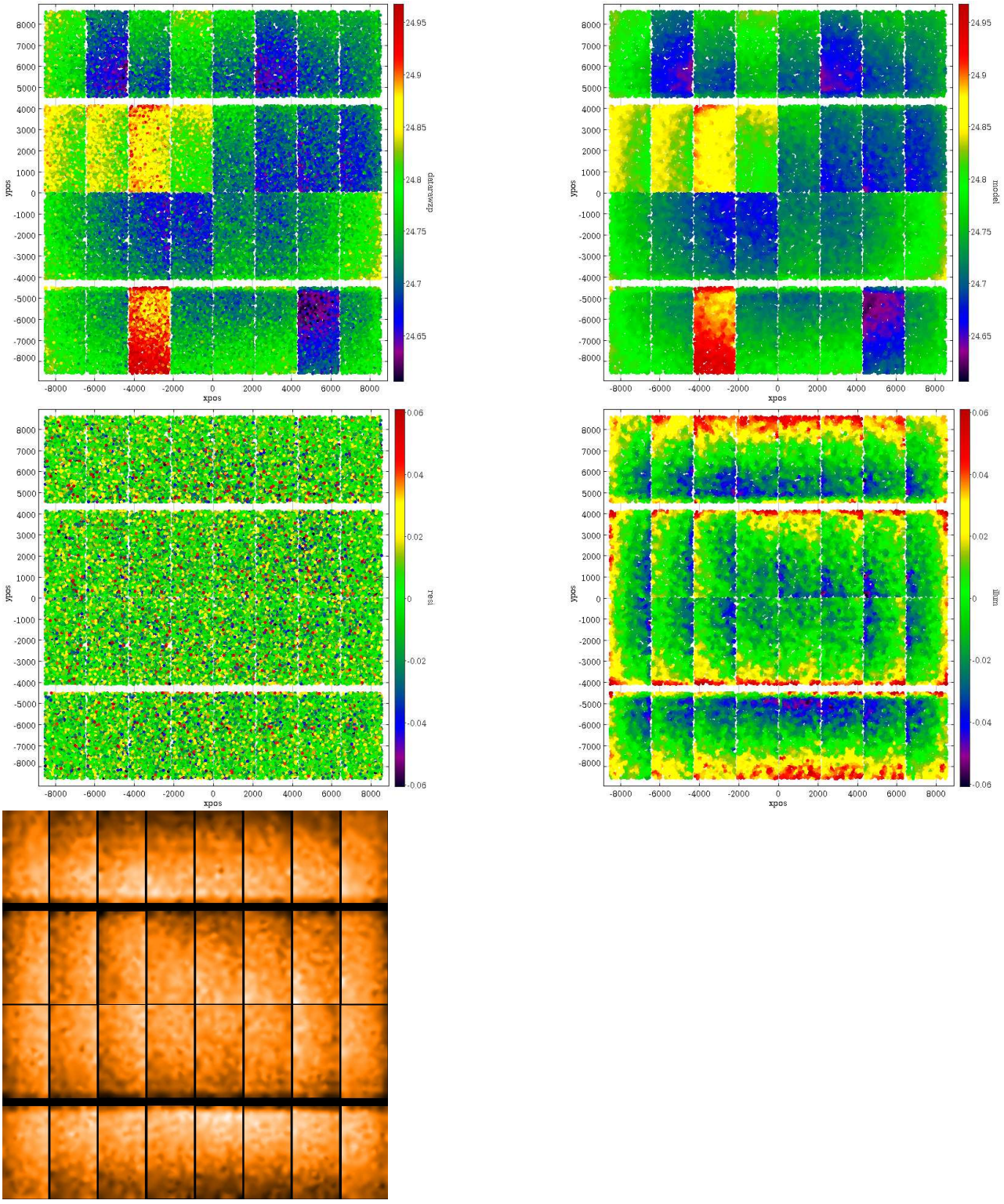

Figure 9: Illumination correction results for Sloan r projected on the focal plane. The datapoints in the top four plots represent all DR7 reference stars of SA92, SA95 and SA113 after dithering 33 times and filtering (see text). Bottom three plots have a color scale from -0.06 to +0.06 magnitude. Data points are enlarged in such a way to fill up gaps, overlapping datapoints should be minimal. Top left: raw zeropoints for all SDSS DR7 reference stars. Top right: model = fitted zeropoints per chip + illumination variation model. Middle left: residual magnitudes of reference stars after applying illumination correction. Middle right: illumination variation model (i.e. with ZPT per chip subtracted). Bottom: full illumination correction model .

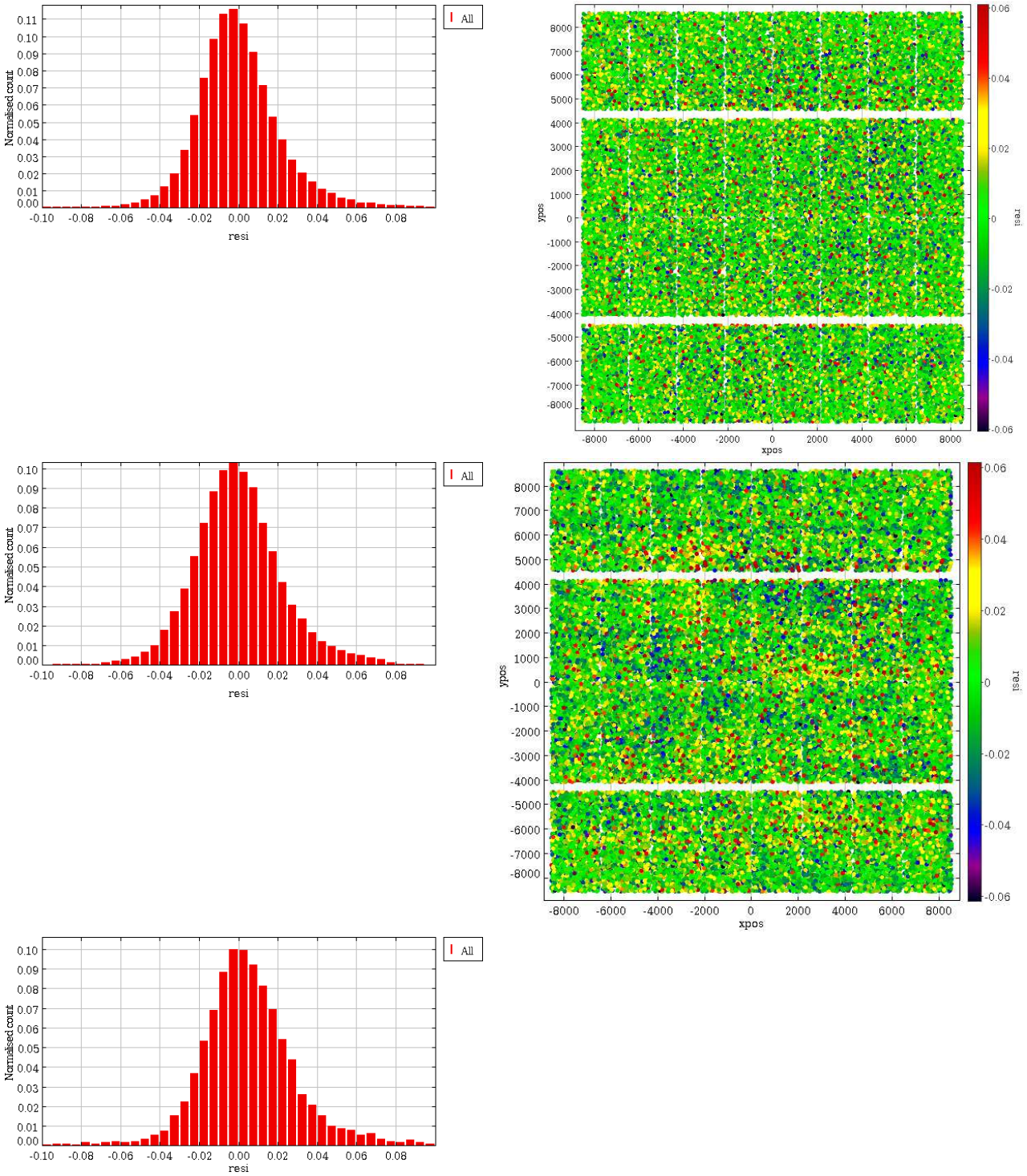

Figure 10: Illumination correction results r band: Top left and right: histogram and focal plane map of residual magnitudes after applying illumination correction on data itself (combination of SA92, SA95 and SA113). Middle: same plots for SA113-data reduced with twilight flatfield rotated -71 degrees compared to the flatfield used to derive the illumination correction. Bottom: same as top plots before but now for KiDS_139.0_-1.5 with template start 2012-02-29 04:33:25 reduced with the same flatfield as the illumination correction (KiDS-mode).

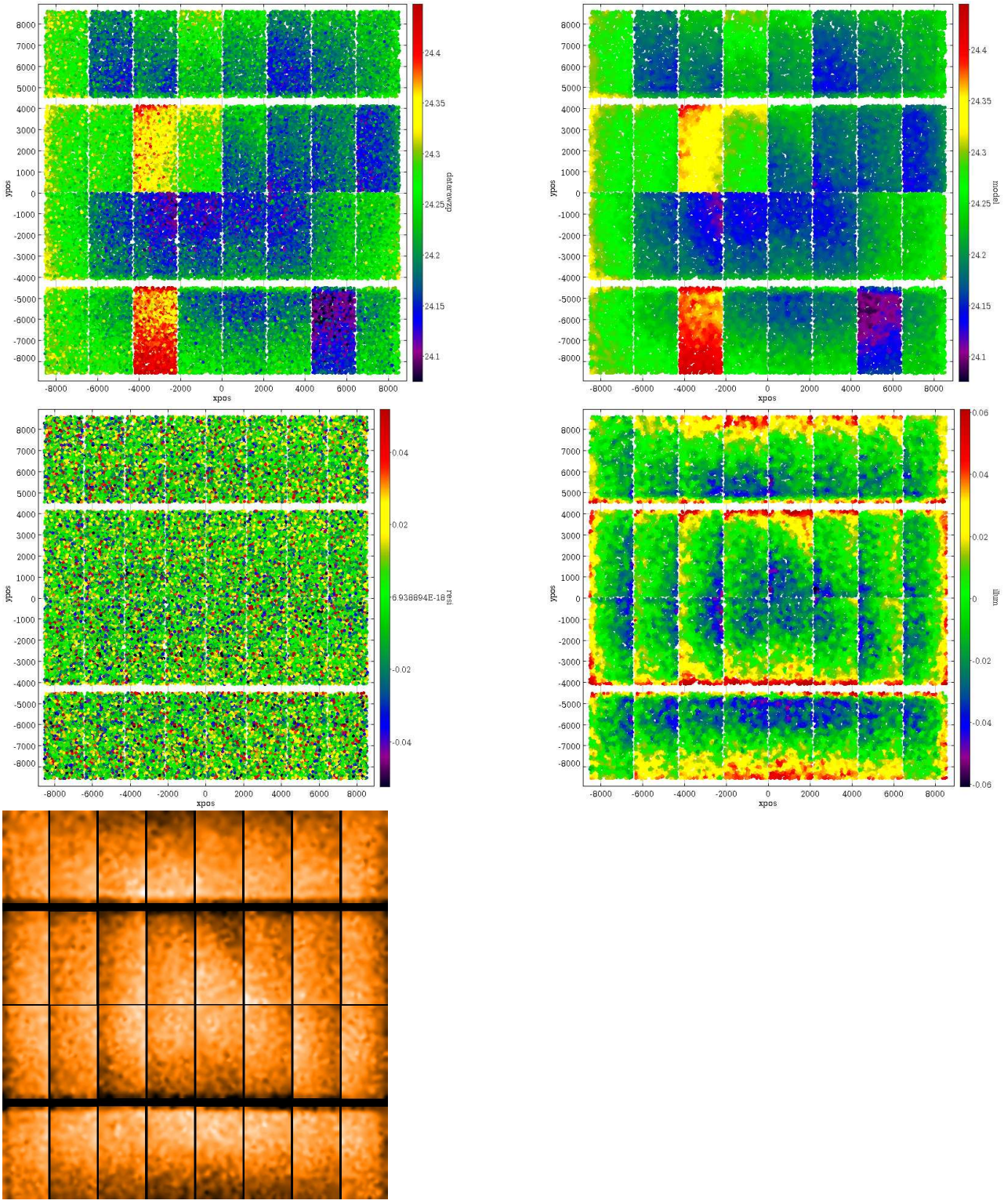

Figure 11: Illumination correction results for Sloan i projected on the focal plane. The datapoints in the top four plots represent all DR7 reference stars of SA92, SA95 and SA113 after dithering 33 times and filtering (see text). Bottom three plots have a color scale from -0.06 to +0.06 magnitude. Data points are enlarged in such a way to fill up gaps, overlapping datapoints should be minimal. Top left: raw zeropoints for all SDSS DR7 reference stars. Top right: model = fitted zeropoints per chip + illumination variation model. Middle left: residual magnitudes of reference stars after applying illumination correction. Middle right: illumination variation model (i.e. with ZPT per chip subtracted). Bottom: full illumination correction model .

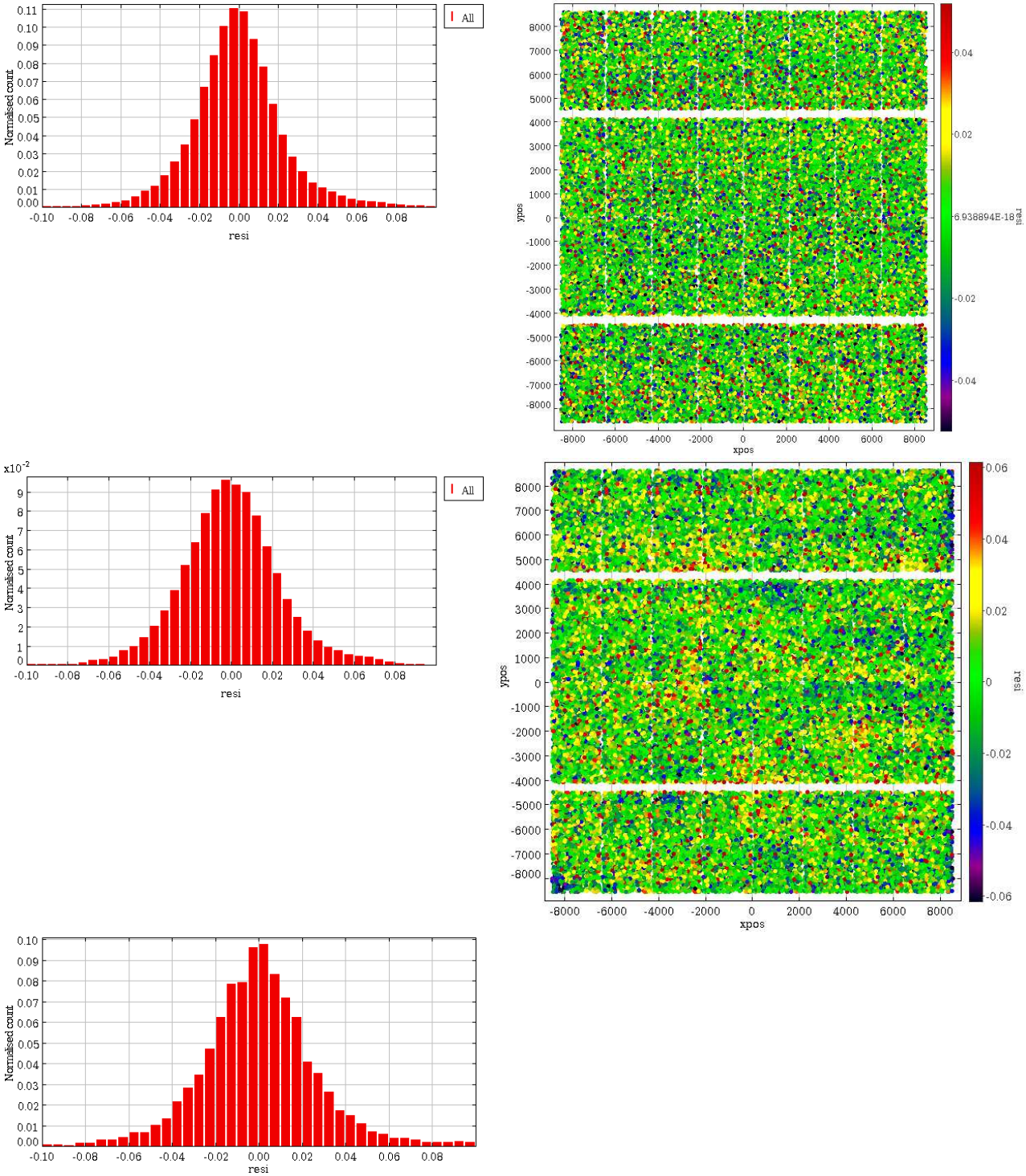

Figure 12: Illumination correction results i band: Top left and right: histogram and focal plane map of residual magnitudes after applying illumination correction on data itself (combination of SA92, SA95 and SA113). Middle: same plots for SA113-data reduced with twilight flatfield rotated -119 degrees compared to the flatfield used to derive the illumination correction. Bottom: same as top plots before but now for KiDS_135.0_0.5 with template start 2011-12-22 06:57:04 reduced with the same flatfield as the illumination correction (KiDS-mode).

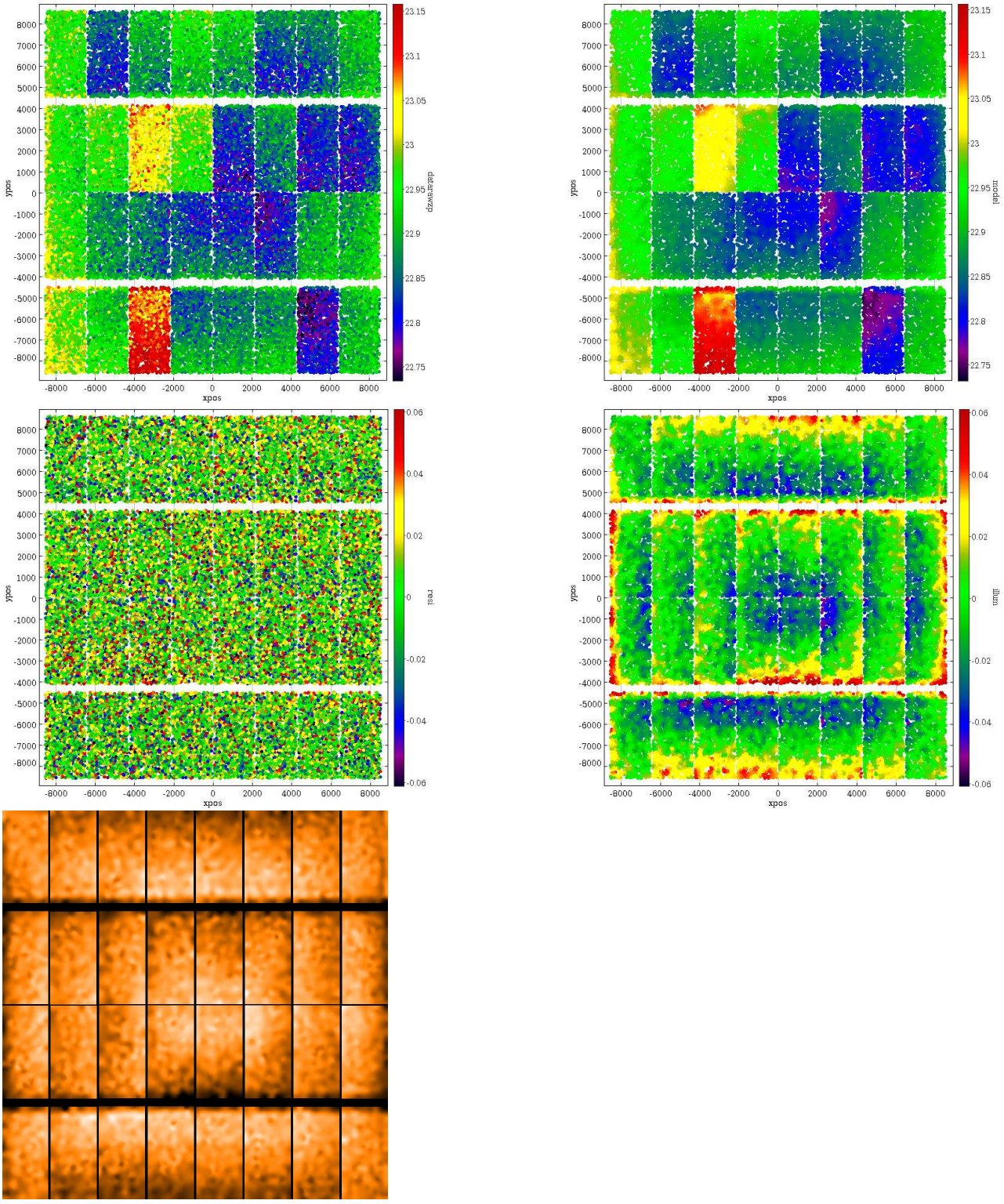

Figure 13: Illumination correction results for Sloan z projected on the focal plane. The datapoints in the top four plots represent all DR7 reference stars of SA92, SA95 and SA113 after dithering 33 times and filtering (see text). Bottom three plots have a color scale from -0.06 to +0.06 magnitude. Data points are enlarged in such a way to fill up gaps, overlapping datapoints should be minimal. Top left: raw zeropoints for all SDSS DR7 reference stars. Top right: model = fitted zeropoints per chip + illumination variation model. Middle left: residual magnitudes of reference stars after applying illumination correction. Middle right: illumination variation model (i.e. with ZPT per chip subtracted). Bottom: full illumination correction model .

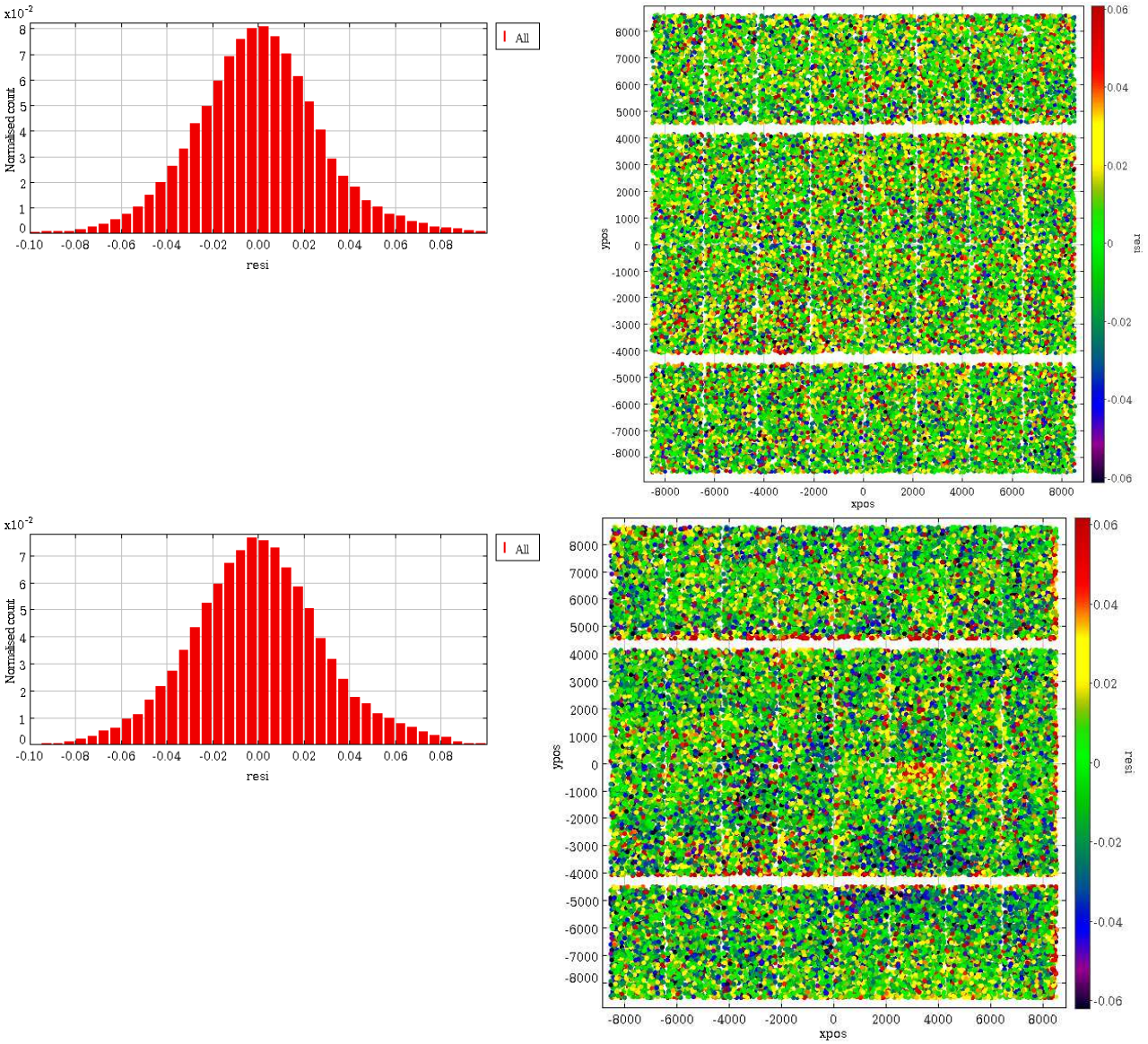

Figure 14: Illumination correction results z band: Top left and right: histogram and focal plane map of residual magnitudes after applying illumination correction on data itself (combination of SA92, SA95 and SA113). Middle: same plots for SA113-data reduced with twilight flatfield rotated 158 degrees compared to the flatfield used to derive the illumination correction.

Abazajian, K. N., Adelman-McCarthy, J. K., Agüeros, M. A., et al., 2009, ApJS, 182, 543
Bertin E., Mellier Y., Radovich M. et al., 2002, in Astronomical Data Analysis Software and Systems XI, ASP Conf. Series 281, 228.
Cappellari, M. & Copin, Y. , 2003, MNRAS, 342, 345
Cappellari, M., astro-ph:0912.1303; 2009, Invited review for the volume "Tessellations in the Sciences: Virtues, Techniques and Applications of Geometric Tilings", eds. R. van de Weijgaert, G. Vegter, J. Ritzerveld and V. Icke, KluwerSpringer)
Koch, A., Odenkirchen, M., Grebel, E. K., Caldwell, J. A. R., 2004AN, 325, 299
Manfroid, J., Selman, F. & Jones, H., 2001Msngr, 104, 16
Regnault, N., 2007, ASPC, 364, 587
Verdoes Kleijn, G.; de Jong, J. T. A.; Valentijn, E. A.; Kuijken, K., 2012, astro-ph-1112.0886